THE ASTROPHYSICAL JOURNAL, **198**: 765–773, 1975 June 15

TYPE I SUPERNOVAE. I. THE He II, He I, H I SPECTRUM, 30 DAYS AFTER THE EXPLOSION

CHARLOTTE GORDON
IBM Thomas J. Watson Research Center, Yorktown Heights, New York
Received 1974 September 3

ABSTRACT

We have computed the He II, He I, and H I spectra (lines and continuum) for a model of Type I supernovae consisting of a spherically expanding shell with a stratification of ionization. We have assumed three different laws for the variation of the density $\rho(v)$ with the expansion velocity v in the shell [$\rho \approx \rho_0(v_0/v)^2$; $\rho \approx \rho_1$, and $\rho \approx \rho_2(v_0/v)^3$], and have determined ρ_0, ρ_1, or ρ_2 by comparison of our theoretical spectrum with the observed spectrum of SN 1972 in NGC 5253 corresponding to the same stage of evolution. Helium is the most abundant element, but hydrogen must be present in the bulk of the ejected material if we want to explain the observed stratification of ionization. The relative abundance of H and He varies with the density law adopted. For all the density models the temperature T_e in the inner layers of the shell must be close to 20,000 K. The expansion of the shell cannot be adiabatic, and our model requires the presence of a neutron star inside the shell.

Subject headings: abundances, stellar — supernovae

I. INTRODUCTION

Different interpretations of Type I supernovae (SN I) have been proposed during the last few years. In the model of Morrison and Sartori (1969) the spectrum is composed only of emission lines formed in a diffuse circumstellar medium (presupernova shell) excited by ultraviolet photons produced during the explosion. Gordon (1972) has interpreted the spectrum as emission and absorption lines over a weak continuum whereas Kirshner *et al.* (1973) have interpreted it as a superposition of emission and absorption lines over a strong continuum. The most recent paper is that of Mustel (1974), who considers only the presence of absorption lines over a continuum.

Calibrated spectra of the Type I supernova SN 1972 in NGC 5253 have been recently published by Kirshner *et al.* (1973). As the distance of NGC 5253 is known to be 4 Mpc (Sersic, Pastoriza, and Carranza 1972), we have for the first time the opportunity to test on absolute data the model of Type I SN shell that we have previously proposed (Gordon 1972*b*). In this model each layer of the shell expands with a velocity v which is proportional to the radius r. The lower velocity is $v_0 \approx 10^8$ cm s^{-1}, and velocities up to $v \approx 2 \times 10^9$ cm s^{-1} exist in the outer layers where the Hα absorption line is formed. Different theoretical models have predicted the existence of such dispersion of velocities (Colgate and White 1966; Hansen and Wheeler 1968) and have also given a variation of the density $\rho(v)$ with the velocity v of the type $\rho(v) \approx v^{-n}$. Using the identification of the different systems of absorption lines, we have shown (Gordon 1972*b*) that a stratification of ionization exists in the shell. Helium, the most abundant element is successively in the state of He^{++} (zone A from a velocity v_0 to a velocity v_1), of He$^+$ (zone B from v_1 to v_2), and of He^0 (zone C from v_2 up to $v \approx 2 \times 10^9$ cm s^{-1}). The He II spectrum is formed by recombination in zone A, the He I spectrum by recombination in zone B. Hα is absent in emission in the late stages of evolution of SN I 1937 in IC 4182 ($t > 275$ days). At that time the shell is optically thin and we see the inner regions of the shell. This lead us to believe (Gordon 1972*b*) that the shell is poor in hydrogen. In this paper we will discuss more precisely the relative abundance of hydrogen and helium and show that hydrogen must be present in the bulk of the ejected material.

Our first set of computations, whose results are given here, corresponds to a time t of 30 days after the explosion. At that date the three ionization zones A, B, and C are defined by the velocities $v_0 \approx 10^8$–1.4×10^8 cm s^{-1}, $v_1 \approx 7.5 \times 10^8$ cm s^{-1}, $v_2 \approx 1.3 \times 10^9$ cm s^{-1} and $v_3 \approx 2 \times 10^9$ cm s^{-1}.

We have computed successively the He II and H I spectra produced in zone A, the He I and H I spectra produced in zone B, the H I spectra produced in zone C for the three density laws $\rho \approx v^{-n}$ with $n = 2$, 0, or 3. Our final model, computed taking in account the absorption in zone B or C of the radiation emitted by zone A, is compared to the observed spectrum of SN 1972 in NGC 5253 corresponding approximately to the same stage of evolution of the SN I shell.

II. GENERAL PROPERTIES OF THE MODEL

The zones A, B, C are ionized by a primary radiation which can be formed around the pulsar or in the innermost regions of the ejected shell (region X) heated to a high temperature T_x by the absorption of magnetic dipole radiation or energetic particles. Our model does not depend upon the way the energy released by the pulsar is transferred to the shell.

a) In zone A, helium is doubly ionized; hydrogen, if present, is totally ionized. The heavy elements C, O, Fe, Mg, . . . are also highly ionized by absorption of the primary radiation. They emit ultraviolet photons ($h\nu > 54$ eV) able to ionize He$^+$. We do not know the abundance of these heavy elements, nor do we know the frequency dependence of the primary radiation, and we cannot compute the degree of ionization of He^+. We introduce a parameter $c = n_1(He^+)/n_e$ where $n_1(He^+)$ is the population of the ground level of He^+ and n_e the electron density. This parameter will characterize the degree of ionization of He^+ in zone A.

We do know that in zone A, the total number of recombinations $n_{rec}(He^{++})$ of He^{++} to He^+ is equal to the total number of photoionizations from He^+ to He^{++}. The recombination time at $t \approx 30$ days is very short for all the density models ($\tau_r \approx 10$–100 seconds) and ionizing photons must be continuously provided to zone A. If the shell is optically thin, we can estimate from $n_{rec}(He^{++})$ the energy furnished to the shell by the neutron star. In zone A, He^{++} will recombine, emitting the He II spectrum. In the absence of H in zone A, the He II Lα and Balmer continuum photons escaping the zone A will ionize He^0 to He^+ in zone B. However, if H is present, a part of these photons will be used to ionize H. The electron temperature T_e in zone A cannot be determined directly from the energy balance since both heating and cooling rates are unknown. T_e is determined empirically from the comparison of the observed and computed spectra.

Zone A is limited by a velocity v_1 corresponding to the blueshift of the absorption line He I $\lambda 5876$ formed in zone B.

b) In zone B, helium is singly ionized by absorption of the primary photons with an energy 24 eV $< h\nu <$ 54 eV and by absorption of the He II Lα and Balmer continuum photons produced in zone A. The total number of recombinations of He^+ to He^0 gives us an upper limit on the number of He II Lα and Balmer continuum photons escaping the zone A. We have assumed that the absorption of photons with an energy $h\nu > 24$ eV is complete in zone B.

He^+ will recombine, emitting the He I spectrum. Lines of He I are observed in emission and in absorption. The opacity of the He I continuum due to absorption from the levels $n = 2$ must be large to explain the lack of ultraviolet ($\lambda < 3500$ Å) emission in the early stages of evolution of the SN. But as we see the He II lines in the visible spectrum, the thickness of zone B at these wavelengths must be smaller than the thermalization length in the He I continuum throughout the visible range. The He I $\lambda 584$ resonance line can be absorbed in zone B to ionize H, or it can escape zone B and ionize H and heavy elements in zone C. In zone B, Na will be ionized to Na^{+2} by absorption of He II Lβ photons and Ca will be ionized to Ca^{+3} by absorption of He II Lγ and Lδ photons.

The He I absorption line $\lambda 5876$ which has a maximum of absorption close to v_1, and disappears at a wavelength corresponding to a velocity $v_2 \approx 1.3\ 10^9$ cm s^{-1}. We have chosen this velocity to limit zone B.

c) In zone C, helium is neutral. The Fe II absorption lines are formed in this zone. The presence of Hα in absorption with a blueshift corresponding to $v \approx 1.9 \times 10^9$ cm s^{-1} (position of the maximum of absorption) shows that H does exist in this zone. Our model must explain this Hα absorption. Our computations show that Hα has a maximum of absorption at the end of zone C (H^+ zone), and we set $v_3 \approx 2 \times 10^9$ cm s^{-1}. In zone C, Ca will be mainly in the state of Ca^{+2} and Na in the state of Na^+. The recombination spectra of Ca II and Na I are formed in that region. The radial velocities corresponding to the maximum of absorption in the Ca II and Na I lines must be similar. The maximum of absorption in the line $\lambda 8600$ of Ca II corresponds to $v \approx 1.3$–1.5×10^9 cm s^{-1} while the maximum of absorption in $\lambda 5890$ of Na I corresponds to $v \approx 8 \times 10^8$ cm s^{-1} if the line in absorption is identified with $\lambda 5730$ (Kirshner *et al.* 1973). The main contribution to the absorption line $\lambda 5730$ must come from He I $\lambda 5876$.

III. STUDY OF THE He^{++} ZONE (ZONE A)

The electron temperature T_e and the degree of ionization of helium (parameter c) are supposed to be constant throughout the zone. The electron density at a velocity v, $n_e(v)$, follows the same law that the mass density $n_e(v) = n_{e,0}(v_0/v)^{-n}$ where $n_{e,0}$ is the electron density in the innermost regions of the shell of velocity v_0; the index n will take successively the values $n = 2$, $n = 0$ and $n = 3$. The hydrogen abundance is characterized by a parameter $[a] = N(H)/N(He)$ where $N(H)$ and $N(He)$ are the total densities of all the helium and hydrogen ions and atoms. Zone A is defined by the four parameters T_e, $n_{e,0}$, c, and $[a]$.

a) *Continuum Spectrum*

Photons are created by free-free ϵ_{ff} and free-bound emission ϵ_{fb} of He^+ and H. They are absorbed by free-free or bound-free absorption of He^+ and H and scattered by Thomson scattering. The total optical depth at each frequency ν is

$$\tau_\nu = \tau_e + \tau_{ff,\nu}(He^+ + H) + \tau_{bf,\nu}(He^+ + H)\,.$$

The optical depth $\tau_{bf,\nu}$ depends upon the populations of the different bound levels of He^+ and H which are solutions of the statistical equilibrium equations relative to He^+ and H.

We have already shown (Gordon 1972*b*) that, at $t = 30$ days, $\tau_e \gg (\tau_{ff} + \tau_{bf})$ in the visible range. The medium will be optically thin at a frequency ν if

$$\tau_\nu{}^1 = \sum_{v_0}^{v_1} \{3\tau_e(v)[\tau_{bf,\nu}(v) + \tau_{ff,\nu}(v)]\}^{1/2} < 1\,.$$

If $\tau_\nu{}^1 > 1$, photons produced in the inner layers of the shell may be destroyed before escaping, and the radiation transfer in the continuum must be solved to know the emerging intensity.

b) *Formation of the Line Spectrum*

The expansion velocity in the shell greatly exceeds the thermal velocity of atoms. The computation of the radiation transfer for line photons is replaced by the computation of their escape probability β by the method introduced by Sobolev (1960), where we have taken in account the increase of velocity $v(r)$ with the radius following the law $r = v(r)t$, where t is the time in seconds elapsed since the explosion. This escape probability β is similar to the simplified probability used by Castor and Van Blerkom (1970).

If $\tau_{\nu_0}{}^1 > 1$, line photons of frequency ν_0 may be absorbed in the continuum. If $v_\nu{}^*$ is the velocity at which $\tau_\nu{}^1 \approx 1$, we suppose that at frequency ν only line photons produced in the layers of velocity $v > v_\nu{}^*$ can escape. The value of $v_\nu{}^*$ corresponds to the integration over zone A only, and in our final model the line intensities will be corrected for the absorption in zone B.

For a transparent shell the total width of the line is $2\Delta\lambda = 2\lambda_0 v_1/c$. However, our computations show that the broadening by Thomson scattering is large, since for most of the models which may be solutions τ_e(zone A) $\approx$ 10–30 and τ_e(zone B) $\approx$ 1–2. For that reason we have computed not the line profiles but only the line total intensities.

c) *Method of Computation*

We divide the shell into layers of thickness $\Delta h = t\Delta v$; and in each layer characterized by the parameters $n_e(v)$, T_e, c, and $[a]$, we solve the statistical equilibrium equations for an He^+ or H atom represented by eight levels and a continuum (Gordon 1972*b*). We have included all the radiative and collisional processes between the levels and continuum. For He^+ we have the value of $n_1(He^+)$ determined by c. For H, the degree of ionization is computed directly in each zone (see § III*e*).

We compute $\tau_\nu{}^1$ for 16 frequencies distributed in the spectrum. If $\tau_\nu{}^1 < 1$ in the visible range, lines and continuum intensities are computed as if the medium were optically thin. This is the case for the models $\rho \approx$ constant ($n = 0$).

If $\tau_\nu{}^1 > 1$ in the visible range, we have to solve the radiation transfer in the continuum. To avoid the complexities of the solution of the radiation transfer for a spherically symmetric atmosphere, we have used the following simplifications which are justified at $t \approx 30$ days when more energy is emitted in the lines than in the continuum.

If $v_\nu{}^* < 2v_0$, we have neglected the variation of the flux with the radius and have considered the inner layers as plane-parallel. The radiation transfer is solved by the linearization method of Feautrier (1964) neglecting the frequency shift of a continuum photon with increasing velocity along the line of sight ($\Delta\nu/\nu < 10^{-2}$). The contribution of the layers of velocity $v_\nu{}^* < v < v_1$ has been computed as if the medium were optically thin; however, we have introduced for the emissivity $\epsilon(v)$ of each layer a correction for occultation:

$$\epsilon(v) = [\epsilon_{\rm ff}(v) + \epsilon_{\rm fb}(v)]A(v)\,,$$

$$A(v) = 1 - W(v) = 0.5[1 + (1 - v_\nu{}^{*2}/v^2)^{1/2}]\,.$$

$W(v)$ is the geometrical dilution factor. We have assumed that the layers with $v < v_\nu{}^*$ are opaque to the radiation coming from the layers where $v > v_\nu{}^*$.

In this category are all the models with a density law. The density $\rho \approx \rho_0(v_0/v)^2$ if ν is in the visible range $\nu \approx 10^{14}$ to 7.5×10^{14} Hz.

If $v_\nu{}^* > 2v_0$, the plane-parallel approximation is not valid any more. As the main source of opacity is Thomson scattering, the source function S_ν in the layer where $\tau_\nu{}^1 = 1$ is equal to the mean intensity $\bar{I}_\nu$ and not to the Planck function $B_\nu(T_e)$. If we can write $\bar{I}_\nu = WB_\nu(T_e)$, where W is a dilution factor (Gordon 1973), we know the shape of the continuum but not its absolute intensity. As the variation of the radius is large in the layers where $\tau_\nu{}^1 < 1$ (larger volume involved), an underestimate of the continuum intensity can be obtained from the emissivity of the optically thin layers of velocity $v > v_\nu{}^*$. This emissivity is corrected for the effect of occultation by the innermost optically thick layers.

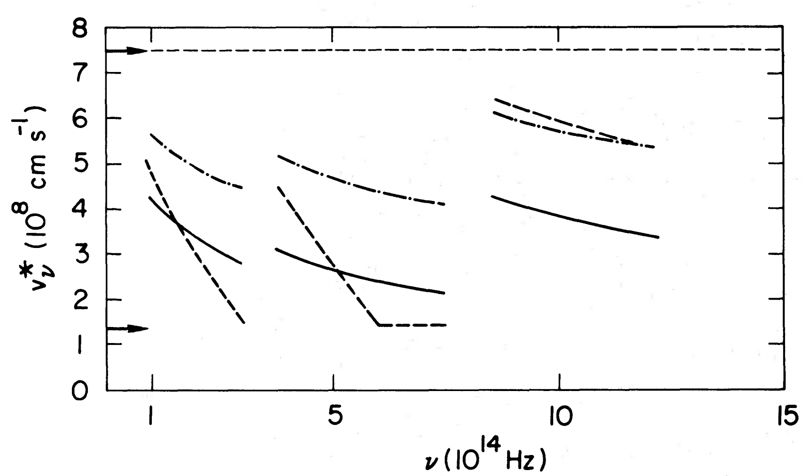

FIG. 1.—Variation of $v_\nu{}^*$ in function of ν for the three models: ———, $\rho \approx v^{-2}$, $n_{e,0} = 2.5\ 10^{11}$, $a = 0.2$, $T_e = 2 \times 10^4$ K, $c = 5 \times 10^{-8}$; – –, $\rho \approx cst$, $n_{e,0} = 10^{10}$, $a = 0.5$, $T_e = 2 \times 10^4$ K, $c = 5 \times 10^{-8}$; –.–, $\rho \approx v^{-3}$, $n_{e,0} = 3 \times 10^{12}$, $a = 0.3$, $T_e = 2 \times 10^4$ K, $c = 10^{-8}$. $v_\nu{}^*$ has only been computed far from a discontinuity limit.

TABLE 1

ZONE A: MODELS IN $\rho = \rho_1(v_0/v)^2$

T_e (10^4 K)	$n_{e,0}$ (10^{11} cm^{-3})	[a]	c	ϕ(5500 Å) (10^{27} ergs cm^{-2} s^{-1})	I(4686) (10^{41} ergs s^{-1})	I(10123) (10^{40} ergs s^{-1})	I(6562) (10^{40} ergs s^{-1})	I(Hα) (10^{40} ergs s^{-1})	N (Lα, He II)	N_{rec} (He$^+$)
2.5	2.5	0	5×10^{-8}	2.8	4.0	6.7	5.3	...	1.4×10^{54}	3.8×10^{52}
2.0	3.0	0	5×10^{-8}	3.8	5.7	8.9	6.2	...	1.8×10^{54}	6.2×10^{52}
	2.5	0	5×10^{-8}	2.8	4.1	6.9	5.3	...	1.4×10^{54}	4.3×10^{52}
	2.5	0	1×10^{-4}	2.1	4.1	5.6	5.9	...	2.0×10^{53}	4.3×10^{52}
	1.8	0	5×10^{-8}	1.9	3.0	5.1	3.7	...	1.2×10^{53}	2.2×10^{52}
1.5	2.5	0	5×10^{-8}	3.4	4.6	7.7	5.8	...	1.6×10^{54}	4.9×10^{52}
2.5	2.5	0.2	5×10^{-8}	2.2	2.7	4.3	3.8	2.2	3.1×10^{52}	3.8×10^{52}
2.0	2.5	0.1	5×10^{-8}	2.7	3.4	5.0	5.7	1.7	5.5×10^{52}	4.3×10^{52}
		0.2	5×10^{-8}	2.4	2.9	4.8	4.3	2.5	3.3×10^{52}	4.3×10^{52}
		0.3	5×10^{-8}	2.2	2.5	4.3	3.2	2.9	2.6×10^{52}	4.2×10^{52}
2.0	1.8	0.2	1×10^{-3}	1.1	2.3	3.3	3.7	1.4	3.1×10^{52}	2.2×10^{52}
		0.2	5×10^{-8}	1.5	2.0	3.4	3.0	1.8	2.1×10^{52}	2.2×10^{52}
		0.3	5×10^{-8}	1.4	1.8	3.1	2.4	2.2	1.5×10^{52}	2.1×10^{52}
1.5	1.05	0.2	1×10^{-7}	0.51	1.6	2.2	2.3	0.98	1.0×10^{52}	8.5×10^{51}

In this category are all our models computed with a density law $n = 2$, 0, or 3 in the far-infrared or ultraviolet. Figure 1 shows the variation of v_ν^* with ν for three of the models studied. The He^{++} zone starts at $v_0' = 1.4 \times 10^8$ cm s^{-1}.

d) *Results for a Shell of Pure Helium*

We have first investigated a series of models following the density law $\rho \approx v^{-2}$. The results relative to some of the models which may be fitting the observed spectrum are in Table 1 ([a] = 0). In column (1) is T_e, the electron temperature of zone A. Column (2) gives the electron density $n_{e,0}$ at $v_0 = 10^8$ cm s^{-1}; column (3) gives [a], the relative abundance of H and He. Column (4) gives the value of c which characterizes the degree of ionization of He$^+$; column (5), the flux in the continuum at $\lambda \approx 5500$ Å. Columns (6)–(8) give the intensities of the three He II lines $\lambda\lambda$4686, 10123, and 6562, corrected for occultation but not for absorption along the line of sight for the models [a] = 0. The correction for absorption has been done only for the models [a] $\neq$ 0. In column (9) is the intensity of Hα for the models [a] $\neq$ 0. In column (10) is the number of He II Lα photons escaping zone A, corrected for occultation and absorption. In the last column is the number of He$^+$ recombinations in zone B computed for the same density model, the same T_e, and assuming $\alpha(\text{He}^+) = \sum_2^\infty \alpha_n(\text{He}^+)$ since the "on the spot" approximation will be used to compute the ionization of He^0 in zone B.

The intensities of the He II lines increase as $n_{e,0}$ increases or T_e decreases. In no case we can match the numbers in the two last columns. The number of He II Lα photons escaping zone A is always larger than the number of photoionizations of He^0 in zone B. Zone A cannot be composed of pure helium. Any increase of the exponent n with v in the density law will increase even more the discrepancy between the two last columns.

In our investigations with a density law $\rho = \rho_0$ we have to add a new parameter, the velocity v_4 at which, following Colgate and White (1966) and Colgate and McKee (1969), the density law shifts from $n = 0$ ($\rho = \rho_0$) to $n = 7$ ($\rho \approx v^{-7}$). We assume that $v_4 > 7.5 \times 10^8$ cm s^{-1}, and in § IV we discuss this assumption. The results are in Table 2. The first 10 columns of Table 2 are similar to the first 10 columns of Table 1. Column (11) gives the value of v_4 for which we have the equality between the number of He II Lα photons escaping zone A and the number of He$^+$ recombinations in zone B.

In all the models the shell is transparent in the visible range for [a] = 0. The value of v_4 corresponding to [a] = 0 will be tested in § IV (opacity of zone B in the visible range).

TABLE 2

ZONE A: MODELS IN $\rho = \rho_0$

T_e (10^4 K)	$n_{e,0}$ (cm^{-3})	[a]	c	ϕ(5500 Å) (10^{27} ergs cm^{-2} s^{-1})	I(4686) (10^{41} ergs s^{-1})	I(10123) (10^{40} ergs s^{-1})	I(6562) (10^{40} ergs s^{-1})	I(Hα) (10^{40} ergs s^{-1})	N (Lα, He II)	v_4 ($\times 10^8$)
2.......	10^{10}	0	1×10^{-4}	2.3	6.8	8.1	1.1	...	4.3×10^{53}	...
2.......	10^{10}	0.2	1×10^{-4}	2.2	6.4	7.8	1.1	3.5	1.3×10^{53}	8.4
	10^{10}	0.2	5×10^{-8}	2.2	3.7	7.5	4.7	3.5	1.1×10^{53}	8.2
2.......	10^{10}	0.5	1×10^{-4}	1.9	5.9	7.5	7.8	5.2	8.3×10^{52}	7.9
	10^{10}	0.5	5×10^{-8}	1.9	3.3	6.5	3.3	5.1	6.3×10^{52}	7.7
2.......	9×10^9	0.5	1×10^{-5}	1.5	4.0	6.7	2.4	4.9	6.9×10^{52}	8.0
2.......	8×10^9	0.5	1×10^{-5}	1.2	3.3	5.5	1.9	4.6	5.6×10^{52}	8.0
2.......	7×10^9	0.5	1×10^{-5}	0.93	2.6	4.3	1.5	3.8	4.9×10^{52}	8.1

TABLE 3

ZONE A: MODELS IN $\rho = \rho_2(v_0/v)^3$

T_e (10^4 K)	$n_{e,0}$ (10^{12} cm^{-3})	[a]	c	$\phi(\lambda 5500$ Å) (10^{27} ergs cm^{-2} s^{-1})	I(4686) (10^{41} ergs s^{-1})	I(10123) (10^{40} ergs s^{-1})	I(6562) (10^{40} ergs s^{-1})	I(Hα) (10^{40} ergs s^{-1})	N (Lα, He II)	$N_{\rm rec}$ (He$^+$)
2......	3	0	10^{-5}	...	4.9	6.0	9.9	...	9.1×10^{53}	6.6×10^{52}
2......	3	0.2	10^{-4}	...	3.6	4.6	7.5	2.8	9.1×10^{52}	6.5×10^{52}
2......	3	0.4	10^{-4}	...	3.3	4.4	6.6	3.7	5.7×10^{52}	6.4×10^{52}
2......	2	0.2	10^{-4}	...	3.4	4.4	5.8	2.2	5.5×10^{52}	3.1×10^{52}
2......	2	0.4	10^{-4}	...	2.9	4.1	5.0	3.2	3.5×10^{52}	3.0×10^{52}
2......	1	0.2	10^{-4}	1.9	2.1	2.9	3.5	1.4	2.4×10^{52}	7.7×10^{51}
2......	1	0.6	10^{-4}	1.7	1.7	2.5	2.6	2.4	1.0×10^{52}	7.3×10^{51}
2......	1	0.6	10^{-8}	1.9	0.84	2.3	1.1	2.4	4.8×10^{51}	7.3×10^{51}

We finally investigate the models where $\rho \approx v^{-3}$. The results are in Table 3, where only one model is included since in no case can we match the two last columns for a shell of pure helium.

e) Results for a Shell Composed of Helium and Hydrogen

The ionization of He$^+$ is always characterized by the same parameter c. We suppose that hydrogen in each layer of velocity v is ionized by He II Lα and Balmer continuum photons produced in the same layer.

The computations are performed as before, computing for each layer of velocity v and electron density $n_e(v)$ the free-free and free-bound emission of He$^+$ and H, the free-free and bound-free absorption of He$^+$ and H. The thermalization length Λ_ν is computed, and a velocity v_ν^* is defined by

$$\sum_{v_\nu^*}^{v_1} [3\tau_e(v)\tau_{\mathrm{abs},\nu}(v)]^{1/2} = 1 \, .$$

At each frequency the value of the optical depth due to true absorption is the summation of the free-free and bound-free absorptions of He$^+$ and H.

Figure 1 shows the variation of v_ν^* with the frequency ν. The introduction of hydrogen increases the opacity for $\lambda < 912$ Å but does not significantly change the opacity in the visible range. For the models following the density law in v^{-2} the equality between the number of He II Lα photons escaping zone A and the number of He$^+$ recombinations in zone B is obtained for $0.1 < [a] < 0.3$. As can be seen from Figure 2, the value of [a] does not depend strongly on the value of c fixing the opacity in the He II Lyman continuum, since at the wavelength of He II Lα the main source of opacity is the Lyman continuum of hydrogen. Zone A is very opaque at $\lambda = 912$ Å, and photons of the He II Balmer continuum will only escape from the last velocity zones ($\Delta v \approx 300$ km s^{-1}). In Table 1 are some of the models computed.

For the models following a density law $\rho \approx \rho_0$ (Table 2) the value of [a] cannot be determined since each value of [a] has a corresponding value of v_4. Only computations of the opacity of the He$^+$ zone in the visible range can tell us which value of v_4 may be solutions.

For the models following the density law $\rho \approx v^{-3}$ the introduction of hydrogen increases the opacity at all wavelengths. The best fit can be obtained for $n_{e,0} = 3 \times 10^{12}$ cm^{-3} with $0.2 < [a] < 0.4$ or $n_{e,0} = 2 \times 10^{12}$ cm^{-3} with $0.2 < [a] < 0.5$. We have omitted in Table 3 the value of the continuous flux at $\lambda \approx 5000$ Å for the models for which the approximation that we used is too rough. The radiation transfer has to be solved for a spherical atmosphere in most of the cases. However, the shell becomes transparent in X-rays; and even if the opacity in the shell is large

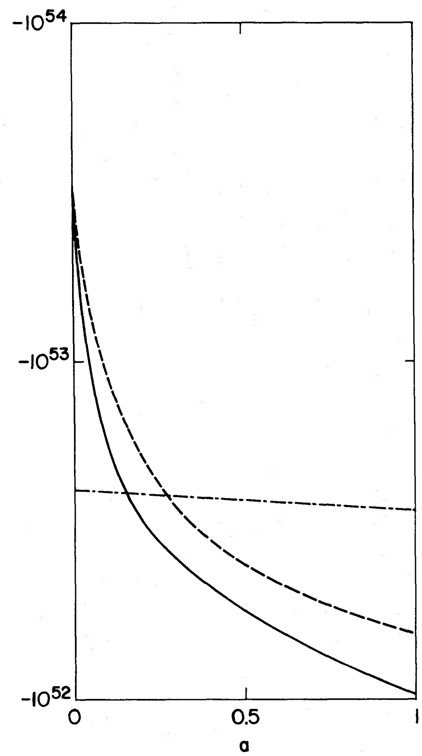

FIG. 2.—Variation of the number of Lα He II photons escaping the zone A with the hydrogen abundance for the model $\rho \approx v^{-2}$, $n_{e,0} = 2.5 \times 10^{11}$, $T_e = 2 \times 10^4$ K, $c = 5 \times 10^{-8}$ (———) or $c = 10^{-4}$ (– – –). The curve (-.-) represents the variation of the number of He$^+$ recombinations in the zone B as a function of the H abundance.

close to 228 Å, He^+ can still be ionized by X-rays of shorter wavelength or by photons of energy $h\nu \approx 54$ eV produced by an indirect process in which X-rays ionize the heavy elements to the stage X^{+n} and ions X^{+n} radiate photons ($h\nu \approx 54$ eV) absorbed on the spot to ionize He^+.

IV. STUDY OF THE He^+ ZONE (ZONE B)

In this zone, helium is ionized by absorption of He II Lα photons escaping zone A. The primary photons with an energy 24 eV < $h\nu$ < 54 eV are absorbed in zone A. Hydrogen is ionized by absorption of He II Balmer continuum photons escaping zone A and by absorption of photons of the line λ584 of He I produced in the same zone.

The degree of ionization of helium in each layer has been computed using the "on the spot" approximation. Each photon emitted in the continuum $n = 1$ of He I is immediately reabsorbed. Singly ionized helium recombines, giving the He I spectrum. The emission in the He I continuum is weak. Our main concern is the opacity of the He I continuum in the visible range or in the ultraviolet ($\lambda < 3500$ Å). In the visible range, the main absorption is the bound-free absorption from the levels $n = 3$ of He or H. In the near-ultraviolet it is the bound-free absorption from the levels $n = 2$ of He I and H, with the principal contribution coming from absorption from the metastable level $2s^3S$ of He I.

We solve the statistical equilibrium equations relative to the different bound levels of He I by the modified Sobolev method already used for He II and H I.

First He I was represented by an atom with 13 levels. We took all levels $n = 1$, $n = 2$, $n = 3$ in the singlet and triplet systems and included one common level $n = 4$ for the singlet, and one level $n = 4$ for the triplet system. But due to the slow convergence of our system of 13 nonlinear equations we have done most of our investigations with a simplified atom of eight levels and a continuum. The eight levels are the singlet levels $1s^1S$, $n = 2$ $(2s\,^1S + 2p\,^1P^o)$, $n = 3$ $(3s^1S + 3p^1P^o + 3d^1D)$, and the triplet levels $2s^3S$, $2p^3P^o$, $3s^3S$, $3p^3P^o$, and $3d^3D$. We put more emphasis on the triplet system since our first computations have shown an overpopulation of the triplet system in comparison with the singlet system even in the presence of the transfer of populations by electron collisions between the singlet and triplet systems. The atomic data and bound-free absorption coefficients are taken from Mihalas and Stone (1968); the spontaneous radiative probability and f-values from Wiese, Smith, and Glennon (1966); the radiative recombination rates from Burgess and Seaton (1960). The free-bound emission of He I was computed using the relation between $\alpha_{n,\nu}(T_e)$ and $\kappa_{\mathrm{bf},n}$ given by Hummer and Seaton (1963).

The collisional excitation rates for the optically permitted transitions have been computed following Van Regemorter (1963). The collisional excitation rates between the different $n = 2$ singlet and triplet levels have been computed with the analytic formula of Mihalas and Stone (1968).

The electron temperature T_e(B) in zone B is assumed to be constant with $T_e(\mathrm{B}) \leq T_e(\mathrm{A})$. The electronic density $n_e(v)$ is deduced from the density $n_{e,0}(v_0)$ adopted for zone A with [a] in the range 0.2–0.3 for the density model in v^{-2}, [a] unknown for the models $\rho \approx \rho_0$, [a] between 0.3 and 0.6 for the models in $\rho \approx v^{-3}$.

For the models $\rho \approx v^{-2}$, the optical depth due to Thomson scattering in zone B is smaller than the optical depth due to true absorption in the near-ultraviolet, $\lambda < 3500$ Å, but is larger than the optical depth due to to true absorption in the visible range.

The lack of ultraviolet radiation from the SN I for $\lambda < 3500$ implies that

$$\sum_{v=v_1}^{v_2} \tau_{\mathrm{abs},\nu}(v) \gg 1 \quad \text{for} \quad \lambda < 3500\text{ Å}\,.$$

As one can see through the B zone in the visible range (presence of He II lines), we have at the corresponding frequencies

$$\tau_\nu{}^1 < 1\,.$$

The results are in Table 4. In column (4) is the value of τ^1 for $\lambda = 5000$ Å. Column (5) gives the value of τ_{abs} for $\lambda = 3000$ Å. In columns (6)–(9) are the total intensities corrected for occultation of the He I lines λλ5876, 10830, 3888, 7665. As the lines λλ5876, 3888 have an absorption component which has not been computed, the intensities quoted in Table 4 are upper limits of the observed intensities. In column (10) is the number of He I λ584 photons available for photoionization of H in zone C. In column (11) is the

TABLE 4

ZONE B: MODELS IN $\rho = \rho_1(v_0/v)^2$

T_e (10^4 K)	$n_{e,0}$ (10^{11} cm^{-3})	[a]	τ^1(5000)	τ(3000)	I(5876) (10^{40} ergs s^{-1})	I(10830) (10^{41} ergs s^{-1})	I(3888) (10^{40} ergs s^{-1})	I(7065) (10^{40} ergs s^{-1})	N(584)	N_{rec}(H$^+$)
2.5....	2.5	0.2	0.72	16.9	3.9	2.5	3.6	4.3	1.4×10^{51}	8.2×10^{50}
2......	2.5	0.2	0.98	27.5	3.8	2.9	4.1	4.8	1.3×10^{51}	8.2×10^{50}
2......	1.8	0.2	0.56	21.0	2.7	2.2	2.2	3.2	8.4×10^{50}	4.3×10^{50}
2......	1.8	0.3	0.58	21.3	2.8	2.3	2.3	3.4	7.8×10^{50}	9.8×10^{50}
1.5....	1.05	0.2	0.38	29.5	1.4	1.7	0.95	2.1	3.9×10^{50}	4.0×10^{50}

TABLE 5

ZONE B: MODELS IN $\rho \approx \rho_0$

T_e (10^4 K)	$n_{e,0}$ (10^{10} cm^{-3})	[a]	v_4 (10^8 cm s^{-1})	τ^1(5000)	τ(3000)	I(5876) (10^{40} ergs s^{-1})	I(10830) (10^{41} ergs s^{-1})	I(3888) (10^{40} ergs s^{-1})	I(7065) (10^{40} ergs s^{-1})	N(584)	$N_{\rm rec}$(H$^+$)
2.5.......	1	0.3	7.7	1.88	18.0	3.9	2.2	6.8	5.6	1.6×10^{51}	1.4×10^{49}
2.5.......	1	0.5	7.7	0.84	11.2	2.8	1.4	3.8	2.9	1.5×10^{51}	3.3×10^{49}
2.........	1	0.5	7.7	1.1	18.0	2.6	1.6	4.0	3.2	1.1×10^{51}	3.3×10^{49}
2.........	0.7	0.5	8.0	1.0	18.5	2.5	1.6	3.6	3.0	7.3×10^{50}	1.6×10^{49}

number of H^+ recombinations in zone C computed for $T_e = 10^4$ K assuming everywhere the same density law, the same value of [a], and zone C limited by $v_3 = 2 \times 10^9$ cm s^{-1}.

The inner regions of the He^+ zone must be at a temperature $T_e \approx (2\text{–}2.5) \times 10^4$ K for the density models adopted. The outer regions of zone B may be at a lower temperature since their contribution to the opacity is small.

In all the models the opacity in the ultraviolet ($\lambda \approx 3000$ Å) is large, and the ultraviolet flux observed by satellite (Holm, Wu, and Caldwell 1974 in the bands at 3320, 2980, and 2460 Å must come from the outer regions of zone B or from zone C (Fe II, Mg II, and Ca II lines) at $t = 30$ days. The escape probabilities β for the four He I lines included in Table 5 are very small throughout zone B for all the computed models. As $\beta \simeq 1/\tau_{\rm line}$, the four lines may have an absorption component on their shortward side corresponding to the absorption by He I of the radiation emitted by zone A. The line λ584 has been corrected for the absorption by the H Lyman continuum along the line of sight.

For the models where $\rho = \rho_0$ until v_4 and $\rho \approx v^{-7}$ thereafter the opacity in the visible range is large and it seems that v_4 is in the range 7.7×10^8 to 8×10^8 cm s^{-1} with a close to 0.5. The intensity of λ5876 is small, and the line λ10830 outside the range of the observed spectra cannot be used as a test of the model. The results are in Table 5.

For the model where $\rho \simeq v^{-3}$, the opacity of zone B is too large for $n_{e,0} = 3.10^{12}$ unless $T_e \simeq 25000$°K. If $n_{e,0} \simeq 2.10^{12}$ cm^{-3}, $[a] \simeq 0.5$ while for $n_{e,0} = 10^{12}$ cm^{-3}, $[a] \simeq 0.6$. The results are in Table 6.

V. STUDY OF THE He^0, H^+ ZONE (ZONE C)

In this zone, helium is neutral, hydrogen is ionized by the absorption of λ584 radiation escaping zone B.

The maximum of absorption in the line Hα occurs at a wavelength corresponding to a radial velocity $v \simeq 1.9 - 2.10^9$ cm s^{-1}. H is present throughout the shell but so heavily ionized that the probability of escape β_{23} is large. Our computations show that β_{23} becomes smaller in the region where the degree of ionization of H decreases, at the limit of the C zone. The temperature T_e (zone C) is assumed to be less than 15000° since helium is neutral in this zone. We have adopted $T_e \simeq 10000$°K. A variation of T_e between 8×10^3 K and 1.2×10^4 K does not change the results.

Our computations start at $v_2 = 1.35 \times 10^9$ cm s^{-1} and can be performed up to $v = 2.35 \times 10^9$ cm s^{-1}. They are stopped at the velocity v_3 where hydrogen becomes mainly neutral since in the outer layers both n_e and T_e are unknown (photoionization of heavy elements such as Fe, Mg, . . .). The model is acceptable if $v_3 \approx 2 \times 10^9$ cm s^{-1}.

For the models in $\rho \approx v^{-2}$, the presence of Hα in absorption can be explained without changing the abundance of hydrogen in the outer layers. While the intensity I(λ584) does not depend strongly on the value of [a], the number of H^+ recombinations $n_{\rm rec}(H^+)$ is proportional to $[a]^2$, and for the models studied $0.2 < [a] < 0.3$.

For the models in $\rho \approx v^{-7}$ in zone C, the intensity of I(584) is so large that H is completely ionized until $v > 2.5 \times 10^9$ cm s^{-1}. No absorption in Hα can be observed even if $[a] = 1$. This assumption is not justified since on the spectrum corresponding to $t \approx 250$ days we have $I(\text{H}\alpha) < I(\lambda 5876 \text{ He I})$. The shell is optically thin at that time, and we have a pure recombination spectrum where $n(\text{H}) < n(\text{He})$. To test our assumption of $v_4 > 7.5 \times 10^8$ cm s^{-1} we have computed models of zones A and B with $v_4 = 5 \times 10^8$ or 6×10^8 cm s^{-1}. In both cases Hα could not be observed in absorption. An increase or decrease of $n_{e,0}$ cannot solve the problem. We are left

TABLE 6

ZONE B: MODELS IN $\rho = \rho_2(v_0/v)^3$

T_e (10^4 K)	$n_{e,0}$(10^{12} cm^{-3})	[a]	τ^1(5000)	τ(3000)	I(5876) (10^{40} ergs s^{-1})	I(10830) (10^{41} ergs s^{-1})	I(3888) (10^{40} ergs s^{-1})	I(7065) (10^{40} ergs s^{-1})	N(584)	$N_{\rm rec}$(H$^+$)
2.5....	3	0.3	1.0	17.7	4.3	2.6	4.7	4.9	1.5×10^{51}	9.5×10^{50}
2......	3	0.3	1.5	31.4	4.3	3.2	5.6	6.0	1.3×10^{51}	9.5×10^{50}
2......	2	0.5	0.7	19.4	2.8	2.2	2.7	3.3	8.1×10^{50}	9.9×10^{50}
2......	1	0.6	0.2	8.9	1.0	1.0	0.59	1.1	3.3×10^{50}	3.3×10^{50}

TABLE 7

FINAL MODELS

n	T_e (10^4 K)	$n_{e,0}$(cm^{-3})	[a]	I(4686) (10^{41} ergs s^{-1})	I(6562) (10^{46} ergs s^{-1})	I(Hα) (10^{40} ergs s^{-1})	I(5876) (10^{40} ergs s^{-1})	I(3888) (ergs s^{-1})	$M/M_\odot$
2.......	2.5	2.5×10^{11}	0.2	1.3	1.4	1.3	3.9	3.6×10^{40}	2.0
	2	1.8×10^{11}	0.2	1.3	2.1	1	2.7	2.2×10^{40}	1.5
	1.5	1.05×10^{11}	0.2	1.0	1.3	1.2	1.4	9.5×10^{39}	0.9
0.......	2.5	10^{10}	0.5	1.5	2.8	1.8	2.8	4.0×10^{40}	0.9
	2	7×10^{9}	0.5	1.0	2.0	1	2.5	3.6×10^{40}	0.6
3.......	2	2×10^{12}	0.5	1.3	2.5	2.2	2.8	2.7×10^{39}	2.1
	2	1×10^{12}	0.6	1.4	2.1	2.2	1.0	5.9×10^{39}	1.0
Maximum "observed" intensity (ergs s^{-1})				6	30	30	20	2×10^{41}	

with the only possibility of an increase of the hydrogen abundance in the outer layers.

If $a \approx 0.5$ in zones A and B, the ratio $n_{\rm H}/n_{\rm He}$ is found to be close to 12 in the outer layers. The value of $n_{\rm He}$ is deduced from the assumption that $dM(v)/dv =$ constant, where $dM(v)$ is the mass of the layers between the velocity v and $v + dv$. Finally for the model in $\rho \approx v^{-3}$ the Hα absorption can be explained without any change of chemical composition in the outer layers. For the model defined by $n_{e,0} = 10^{12}$ cm^{-3}, the Hα absorption is rather weak.

VI. MODEL OF THE SUPERNOVA SHELL, COMPARISON WITH THE OBSERVATIONS

Our final models are computed taking in account the absorption occurring in zone B over the radiation emitted by zone A. The intensities of the main lines are in Table 7 where in column (1) is the exponent n of the density law. The observed spectra (Kirshner *et al.* 1973) are published in a logarithmic scale (log ϕ_ν, log ν), where ϕ_ν is the flux observed at the Earth. We have transformed them in a scale (F_ν, ν) where F_ν is the flux at the supernova, assumed to be at a distance of 4 Mpc. We have compared our results with the spectrum relative to the JD 2,441,461. The comparison is done in the following way: For each density model, we place the continuum at the value given by our theoretical model (Fig. 3) and we then estimate, by numerical integration, the total observed intensity of the lines. Most of the lines are blended or modified by absorption. We have taken into account the presence of blends whenever possible, but in most of the cases we can only deduce from the observations an upper limit to the line intensity. Among the He II lines λ4686 is blended with C III λ4647 formed in zone B. Its longward wing, according to our computations, is only slightly affected by Hβ absorption. Its intensity lies between 6×10^{41} ergs s^{-1}, a value corresponding to the total observed band, and approximately 1.5×10^{41} ergs s^{-1}, a value corresponding to a Doppler width due to the expansion velocity in zone A. The composite line λ6562 He II + Hα is also blended on its shortward side with a line which could be [Fe X] λ6374. The maximum intensity reached by the line is (2.5–3) $\times 10^{41}$ ergs s^{-1}. The He II λ10123 line is at the limit of the recorded spectra, and only its shortward wing is observed. The line is weak with a total intensity in the range 10^{40}–5×10^{40} ergs s^{-1}. Among the He I lines λ5876 is affected by a blend on its longward side where a shoulder is visible on the spectrum. The maximum intensity is of the order of 2×10^{41} ergs s^{-1}. The maximum intensities associated with the bands λ7065 and λ3888 are respectively I(λ7065) $\approx 1.5 \times 10^{41}$ ergs s^{-1} and I(λ3888) $\approx 2 \times 10^{41}$ ergs s^{-1}.

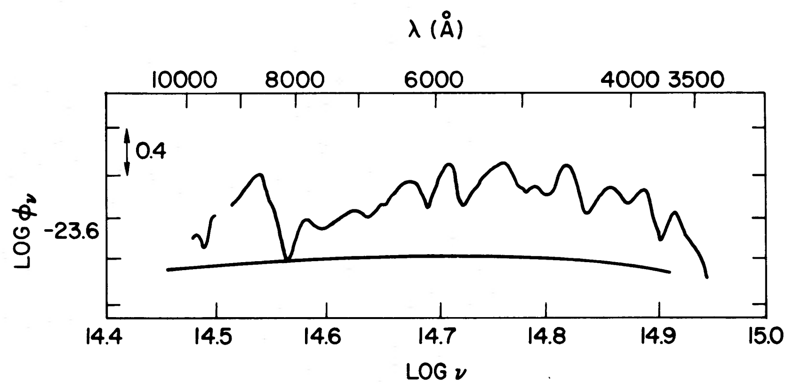

FIG. 3.—Position of the continuum on the observed spectrum for the model $T_e = 2.5 \times 10^4$ K, $n_{e,0} = 2.5 \times 10^{11}$ cm^{-3}, $\rho \approx v^{-2}$, $a = 0.2$. The units are the units used by Kirshner *et al.* (1973).

The comparison between observed and theoretical spectra is difficult in the presence of so many blends, and we can only eliminate the models giving a too high or too weak intensity of some of the lines.

For the models following the density law $\rho \approx \rho_0(v_0/v)^2$ the best fit is obtained for $1.8 \times 10^{11} < n_{e,0} < 2.5 \times 10^{11}$ cm^{-3}. The line λ4686 is perhaps weak, but any increase of $n_{e,0}$ increases the opacity of zone B and the line intensity does not change significantly. The other He II and He I lines have also a theoretical intensity smaller than the observed intensity. They are probably blended.

For the models following the density law $\rho = \rho_1$ until v_4 the intensity of the He II lines depends upon the degree of ionization of He^+ in zone A (Table 2). Tentatively we have assumed that He^+ is ionized only by the primary radiation with $c \approx 10^{-5}$. The corresponding line intensities are in Table 7. In this case also the He II and He I lines must be blended.

For the model following the density law $\rho = \rho_2(v_0/v)^3$ the He II and He I lines must also be blended.

VII. CONCLUSION

Our theoretical computations of the He II, He I, and H I spectra show that we can reproduce the observed spectrum. The large opacity of zone B makes difficult any increase of the theoretical intensities. As the distance of NGC 5253 is only approximately known, the study of the evolution of the spectra with time will tell us if the distance determined by Sersic *et al.* (1973) is slightly underestimated or if important blends do exist at the position of the He II and He I lines.

The densities in the inner layers of the shell are very different for the three density laws investigated. Later in the evolution ($t \geq 250$ days) as the shell expands, the inner layers of the shell are the only layers ionized (Gordon 1972*a*). A study of the forbidden lines observed at that time can give one a clue to determine the density in the inner layers and consequently to determine the density law existing in the inner layers of the shell.

The relative abundance of hydrogen and helium in the shell varies with the density law adopted, but in all cases helium is more abundant than hydrogen. The Balmer lines of H are weak. The models $\rho = \rho_1(v_0/v)^2$ and $\rho = \rho_2(v_0/v)^3$ have a homogeneous ratio [H]/[He], but the models $\rho = \rho_0$ require a higher hydrogen content in the outer layers to explain the Hα absorption. The temperature T_e is mainly determined by the He I opacity in zone B (visible range). A decrease in the central density n_{e0} will lead to a decrease of T_e but also to a decrease of the theoretical intensities of the lines (more important blends). A smooth increase of the exponent n with the velocity v in the density law $\rho \approx v^{-n}$ will also lead to a lower T_e.

The mass of the ejected shell varies with the density law adopted. The masses corresponding to the density law in $\rho \approx v^{-n}$ with $n = 2$ or 3 have been computed assuming a change in the density law at $v_3 = 2 \times 10^9$ cm s^{-1}. We adopt for $v > v_3$ a density law $\rho \approx v^{-7}$. The value of the masses obtained, for our final models are in the range 0.6–2 $M_\odot$ (Table 7).

REFERENCES

Burgess, A., and Seaton, M. J. 1960, *M.N.R.A.S.*, **121**, 471.
Castor, J. I., and Van Blerkom, D. 1970, *Ap. J.*, **161**, 485.
Colgate, S. A. 1970, private communication.
Colgate, S. A., and McKee, C. 1969, *Ap. J.*, **157**, 623.
Colgate, S. A., and White, R. H. 1966, *Ap. J.*, **143**, 626.
Feautrier, P. 1964, *C.R. Acad. Sci. Paris*, **258**, 3189.
Gordon, C. 1972*a*, *Astr. and Ap.*, **20**, 79.
———. 1972*b*, *ibid.*, p. 87.
———. 1973, *ibid.*, **29**, 123.
Hansen, C. J., and Wheeler, J. C. 1968, *Ap. and Space Sci.*, **3**, 464.
Holm, A. V., Wu, C. C., and Caldwell, J. J. 1974, preprint.
Hummer, D. G., and Seaton, M. J. 1963, *M.N.R.A.S.*, **127**, 217.
Kirshner, R. P., Oke, J. B., Penston, M. V., and Searle, L. 1973, *Ap. J.*, **185**, 303.
Mihalas, D., and Stone, M. E. 1968, *Ap. J.*, **151**, 293.
Morrison, P., and Sartori, L. 1969, *Ap. J.*, **158**, 541.
Mustel, E. R. 1974, *Soviet Astr.—AJ*, **17**, 711.
Nussbaumer, H. 1971, *Ap. J.*, **170**, 93.
Sersic, J. L., Pastoriza, M., and Carranza, G. 1972, *Ap. and Space Sci.*, **19**, 469.
Sobolev, V. V. 1960, *Moving Envelopes of Stars* (Cambridge: Harvard University Press).
Van Regemorter, H. 1963, *Ap. J.*, **136**, 906.
Wiese, W. L., Smith, M. W., and Glennon, B. M. 1966, *Atomic Transition Probabilities* (NSRDS–NBS 4), Vol. **1**.

CHARLOTTE GORDON: 60 East 8th Street, New York, NY 1003